Solid Earth Discuss., 7, 537–563, 2015
www.solid-earth-discuss.net/7/537/2015/
doi:10.5194/sed-7-537-2015

Solid Earth Discussions
Open Access

Revealing the deeper structure of the end-glacial Pärvie fault system in northern Sweden by seismic reflection profiling

O. Ahmadi[1], C. Juhlin[1], M. Ask[2], and B. Lund[1]

[1]Department of Earth Sciences, Uppsala University, Villavägen 16, 75236 Uppsala, Sweden
[2]Department of Civil, Environmental and Natural Resources Engineering, Luleå University of Technology, 971 87 Luleå, Sweden

Received: 22 December 2014 – Accepted: 8 January 2015 – Published: 4 February 2015

Correspondence to: O. Ahmadi (omid.ahmadi@geo.uu.se)

Published by Copernicus Publications on behalf of the European Geosciences Union.

Abstract

Fault scarps that extend up to 155 km and have offsets of tens of meters at the surface are present in the northern parts of Finland, Norway and Sweden. These fault scarps are inferred to have formed during earthquakes with magnitudes up to 8 at the time of the last deglaciation. The Pärvie fault system represents the largest earthquake so far documented in northern Scandinavia, both in terms of its length and its calculated magnitude. It is also the longest known glacially induced fault in the world. Present-day microearthquakes occur along the length of the fault scarp on the eastern side of the scarp, in general agreement with an east dipping main fault. In the central section of the fault, where there is a number of subsidiary faults east of the main fault, it has been unclear how the earthquakes relate to the faults mapped at the surface. A seismic profile across the Pärvie Fault system acquired in 2007, with a mechanical hammer as a source, showed a good correlation between the surface mapped faults and moderate to steeply dipping reflectors. The most pronounced reflector could be mapped to about 3 km depth. In an attempt to map the fault system to deeper levels, a new 22 km long 2-D seismic profile which followed the 2007 line was acquired in June 2014. For deeper penetration an explosive source with a maximum charge size of 8.34 kg in 20 m deep shot holes was used. Reflectors can now be traced to deeper levels with the main 65° east dipping fault interpreted as a weakly reflective structure. As in the previous profile, there is a pronounced strongly reflective 60° west dipping structure present to the east of the main fault that can now be mapped to about 8 km depth. Extrapolations of the main and subsidiary faults converge at a depth of about 11.5 km where current earthquake activity is concentrated, suggesting their intersection has created favorable conditions for seismic stress release. Based on the present and previous seismic reflection data, potential locations for future boreholes for drilling into the fault system are proposed.

SED
7, 537–563, 2015

1 Introduction

During the last glaciation the ice that covered much of northern Europe, with thickness in excess of 3 km, gave rise to dynamic changes in the stress field of the Fennoscandian Shield (Pascal et al., 2010). Towards the end of the glaciation, the ice melted rapidly in northern Fennoscandia and the effective stress field changed accordingly, generating major faulting (Lagerbäck, 1978) with associated large earthquakes (M = 7–8.2; e.g. Muir-Wood, 1989; Arvidsson, 1996; Lindblom et al., 2014). The resulting fault scarps have been alternatively termed end-, post- or glacially-induced fault scarps; we use the first term in this paper as it is appropriate for the Pärvie fault.

End-glacial fault scarps are present at a minimum of 14 known locations in Finland, Norway and Sweden and are up to 155 km in length, with a maximum surface displacement of up to 30 m (Kuivamäki et al., 1998; Olesen et al., 2004; Lagerbäck and Sundh, 2008). They generally strike in the NE–SW direction, dip toward the southeast and show reverse faulting motion. The longest of the scarps, located in northern Sweden, belongs to the Pärvie fault system and it has been the focus of recent geophysical studies (Fig. 1), including reflection- and hydroacoustic seismic surveying (Juhlin et al., 2010; Vogel et al., 2013), a temporary seismic network (Lindblom et al., 2014), and remote sensing (Mantovani and Scherneck, 2013).

Important questions concerning the end-glacial faults are (i) what is the geometry of the faults at depth, (ii) what was the stress field that caused these ruptures during the last deglaciation, and (iii) what is the stress field at depth that is generating the current earthquake activity along the faults. Knowledge of the fault geometry is important for understanding the stress required to activate the faults during the last deglaciation and also for predictions of potential future earthquakes along these faults (e.g. Lund et al., 2009). A recent reflection seismic survey across the Pärvie fault system west of the city of Kiruna showed that the faults comprising the system have moderate to steep dips and planar geometries down to at least 2–3 km depth (Juhlin et al., 2010).

SED
7, 537–563, 2015

Similar geometries were found for faults belonging to the Burträsk fault system further to the southeast (Juhlin and Lund, 2011). The more sub-horizontal reflections from the area were interpreted as possibly originating from deeper lying greenstones or gabbroic bodies. The main east dipping Pärvie fault was not very reflective in contrast to a parallel west dipping subsidiary fault within the system. Juhlin et al. (2010) suggested that the Pärvie fault system could represent a flower structure, and concluded that it is unlikely that the main fault becomes listric above 6 km depth. Mapping of brittle deformation structures on outcrops in the area of the main fault also indicate relatively steep dips in the near surface (Riad, 1990).

To investigate an end-glacial fault at depth and help unravel the stress history of northern Fennoscandia, the Drilling into Active Faults in Northern Europe (DAFNE) project has been initiated (Kukkonen et al., 2010, 2011). Deep research boreholes to depths of 2–3 km are planned in order to better understand the present-day stress field and the seismicity associated with the faults, as well as studying the geology, fluids, gases and microbes in the end-glacial faults. The DAFNE project is part of the Swedish Scientific Drilling Program (www.ssdp.se) and the International Continental Scientific Drilling Program (www.icdp-online.org). The reflection seismic survey presented in Juhlin et al. (2010) was a first step in order to optimally locate a deep borehole into the fault system.

In this paper, we present results from a new seismic survey across the Pärvie fault system, which was acquired in June 2014 using a more powerful dynamite source, but with a sparser spacing between the source points and with longer offsets. The Juhlin et al. (2010) survey used an industrial hydraulic hammer as a seismic source. Several kilograms of explosives in deep shot holes will generally generate seismic signals that penetrate deeper than a surface operated hammer. Therefore, it was expected that the new survey would verify the geometry of the main Pärvie fault and allow mapping of the subsidiary faults to deeper levels in the crust, but with a lower resolution image of the uppermost few kilometers. This was indeed the case and together with re-migrated sections of the previous data with the velocity model obtained from Lindblom

SED
7, 537–563, 2015

et al. (2014) we show that the highly reflective west dipping subsidiary fault can be mapped down to at least 7.5 km and that it has a planar geometry with this velocity model. The main Pärvie fault is still not clearly imaged even with the more powerful seismic source, suggesting that it does not have a strong impedance contrast to the surrounding rock.

2 Tectonics and seismicity of the area

The Pärvie fault is located in the intraplate Baltic Shield, mostly in Paleoproterozoic rock on the boundary to the Archean terrain of northernmost Sweden. It runs parallel with, and only some 10–50 km away from the Ordovician Caledonian mountain front. The establishment of permanent seismic stations in northern Sweden in 2003–2004, as part of the Swedish National Seismic Network (Bödvarsson and Lund, 2003), showed that the Pärvie fault, and the other end-glacial faults in northernmost Sweden, are still seismically active. In fact, 70 % of the earthquakes recorded north of 66° N since 2003 locate within 30 km to the southeast and 10 km to the northwest of an end-glacial fault, consistent with the observed reverse faulting, dip to the southeast, character of the faults (Lindblom et al., 2014). Between 2007 and 2010 a temporary network of seismic stations was operated along the Pärvie fault, bringing the number of stations in the vicinity of the fault to 15. Although still sparse for a 155 km long fault, the temporary network significantly improved the detection threshold and location accuracy along the fault. After dismantling of the temporary stations in 2010, two of these were converted into permanent stations in order to continue an improved long term monitoring of the fault. Lindblom et al. (2014) analyzed the earthquakes recorded along the Pärvie fault between 2003 and 2013. The epicentral locations (Fig. 1) show that the earthquakes occur all along the mapped fault scarp, mostly on the eastern side of the fault in accordance with an east dipping reverse fault. In the southern section, and even more pronounced in the northern section (not shown in Fig. 1), the events are located at some distance from the fault scarp whereas in the central section of the

SED
7, 537–563, 2015

fault earthquakes occur closer to the main fault, seemingly bounded by the main fault and a west dipping subsidiary fault. Cross-sections show that events generally tend to occur deeper to the east, although there are still too few events to see a well defined fault zone dipping to the east, if that is the case. The dip of the zone of earthquakes is somewhere between 30 and 60°, more shallow to the north and south, and steeper in the center, as indicated in Fig. 1. Events are recorded down to 35 km depth. Assuming that the currently active zone of earthquakes outline the fault that ruptured 10 000 years ago, that event is estimated to have had a magnitude of 8.0±0.4 (Lindblom et al., 2014). Since, 2003, no event larger than magnitude 2.9 has been recorded along the fault and the largest known event was a magnitude 3.7 in 1967.

At four locations along the main Pärvie fault recent investigations on outcrop scale of the kinematics of brittle deformation structures identify four paleostress fields (Bäckström et al., 2013): three of the paleostress fields are also found in other major shear zones in the area (e.g. Edfelt et al., 2006), whereas the fourth, and most recent field, seems to be unique for the Pärvie fault. This structure indicates a reverse stress field with a strike-slip component (A. Bäckström, personal communication, 2014).

On the larger scale the stress field in Fennsocandia is suggested to be dominated by ridge-push (e.g. Gregersen, 1992; Lund and Zoback, 1999; Slunga, 1991) with contributions from glacial isostatic stress redistribution, sediment loading, topography and erosion (Bungum and Lindholm, 1997). In the north, the stress field is poorly known at depths below 500 m. The World Stress Map has no other stress indicators than single focal mechanisms below 500 m (there are only 6 data points onshore north of 65° N) and they show both reverse and normal faulting conditions, with *P*-axes directions mostly in a general E–W direction, albeit with large variations (Heidbach et al., 2008). Preliminary investigations of the focal mechanisms obtained with the temporary seismic network on the Pärvie fault also show a large variation in focal mechanisms, most are, however, strike-slip to reverse, with a general NW–SE direction of the P-axes (Lindblom and Lund, 2011), consistent with a ridge-push derived stress field.

SED
7, 537–563, 2015

Although the earthquake data show a general deepening of the seismicity to the east, there are few events below 20 km depth and the geometry of the main fault at depth is still uncertain. In the central section of the fault, where there are a number of subsidiary faults and where the previous and current seismic lines are located, the geometry seems even less well defined from the earthquake data. Deeper imaging of the fault by reflection seismic methods can therefore provide important constraints on both the fault and the interaction with the subsidiary faults.

3 Seismic acquisition

In order to resolve the geometry of the Pärvie fault system deeper than the previous studies (Juhlin et al., 2010), a new seismic survey in the area was acquired in June 2014 using an explosive source. A number of studies in Sweden indicate that 10 kg of explosives is sufficient to image the crust down to Moho depths (Juhojuntti and Juhlin, 1998; Juhojuntti et al., 2001; Juhlin et al., 2002). Therefore, we used dynamite as a seismic source with a maximum charge size of 8.34 kg in 20 m deep shot holes. In some shots, because of logistical problems, a minimum charge size of 2.78 kg of the explosive was used. Table 1 shows the acquisition parameters which were used in the seismic survey. The seismic profile was laid out almost in the same location as the previous survey (Juhlin et al., 2010) (see Fig. 1). The acquisition was carried out with an end-on array. To obtain good coverage for seismic imaging, each shot was repeated three times for different spreads along the profile, reusing shot holes on the repeat shots. Nominal shot spacing was 400 m, but 15 shots had to be skipped because the shot holes had collapsed after previous explosions in them. Receiver spacing was 25 m with single 10 Hz geophones deployed during the recording. The data were acquired with a sampling rate of 1 ms and total recording length was 25 s, allowing us to investigate deep structures. Signal-to-noise ratios are high in the data, but the shot and receiver spacing used in the acquisition resulted in a sparse data set (Fig. 2).

SED
7, 537–563, 2015

4 Seismic data processing

Field SEGD files were converted to SEGY format and then sorted by source location along the profile. The geometry of the survey was configured and a straight CDP line was chosen for processing (Fig. 2). An inner trace mute was applied and refraction static corrections were performed to improve the coherency of the gathers. First arrivals became better aligned after applying the refraction static correction (Fig. 3a and b). In an attempt to balance seismic traces and to attenuate ringing signals a spectral balancing filter (10-20-100-150 Hz) was applied. Spherical divergence corrections and band pass filtering (10-20-100-150 Hz) were also performed in the pre-stack processing. Residual static corrections were calculated in a further attempt to increase the coherency of the reflections, but without significant improvement. An FX-Decon filter with a window length of 7 traces was used to enhance linear reflectivity of the reflections in the pre-stack domain. Figure 4a and b shows a shot gather before and after applying the FX-Decon filter, a linear reflection is enhanced which intersects the surface at about receiver peg 105. Time variant filtering and velocity analysis were also carried out before stacking. An NMO correction with a high constant velocity of 13 000 $m\,s^{-1}$ resulted in the best image of the dipping structures in the subsurface (Fig. 5). Attempts to perform dip move-out (DMO) corrections were not successful, most likely due to the sparsity of the data and low fold in the offset gathers. To enhance the reflections on the stacked section, a post-stack FX-Decon filter, with a window length of 7 traces, and a band-pass filter (15-25-90-120 Hz) were applied. Finally, the reflections were migrated to their approximate true locations using the Stolt migration method with a constant velocity of 6000 $m\,s^{-1}$ and depth-converted using a variable velocity extracted from 3-D local earthquake tomography (Lindblom et al., 2014) (see Fig. 6). Table 2 shows the processing steps which were applied to this dataset. Furthermore, to have more constraints on resolving the geometry of the faults, we re-migrated two portions of the Juhlin et al. (2010) data using the gradient velocity model from the 3-D

SED
7, 537–563, 2015

local earthquake tomography (Fig. 7). The seismic sections were then depth-converted with the same velocity model.

5 Interpretation

The conventional processing results show a strong west dipping reflection on the stacked section which can be extrapolated to the surface to about CDP 1300 (reflection R1 in Fig. 5). This reflection appears to be relatively planar and can be traced down to a depth of about 8 km on the migrated and depth converted section (Fig. 6). Juhlin et al. (2010) linked this strongly reflective structure to a west dipping subsidiary fault in the Pärvie fault system (Lagerbäck and Sundh, 2008). Although weak, a trace of the main Pärvie fault was recorded and enhanced in the pre-stack and the post-stack seismic processing (Figs. 3 and 4). Figure 3 shows a shot gather in which a linear reflection has been enhanced and appears to intersect the surface at receiver peg 105, close to the location of the main Pärvie fault (Fig. 2). Based on the previous geophysical and geological studies, the main fault dips to the southeast (Juhlin et al., 2010; Lagerbäck and Sundh, 2008) (see Fig. 7a) which is also consistent with the weak reflection marked by R3 in Figs. 5 and 6. In addition, another planar west dipping reflection is observed further east on the profile and can be traced from 3.5 km down to 7 km depth (reflection R4 in Fig. 6). A reflection corresponding to this feature was also observed on the previous profile (Juhlin et al., 2010), but could only be mapped down to 2–3 km depth. It was interpreted as a previously unknown end-glacial fault belonging to the Pärvie fault system, which subsequently has been identified in new LiDAR data (Mikko et al., 2014). Based on the re-migrated sections of the previous survey shown in Fig. 7, the true dips for reflections R1 and R3 are interpreted to be 60 and 65°, respectively. A dip for reflection R4 was not calculated, but is on the same order as that for reflection R1, assuming that the structure generating it is close to perpendicular to the profile.

SED
7, 537–563, 2015

In addition to the more steeply dipping reflections, some more sub-horizontal reflections are observed at depths of about 7.5 km or deeper (see the two ellipses in Fig. 6). Juhlin et al. (2010) suggested, based on seismic forward modeling, that the shallower sub-horizontal reflections on the previous profile could correspond to the top of mafic or ultramafic intrusions at depth. A similar interpretation may be made for these deeper sub-horizontal reflections.

5.1 Reflectivity of the faults

The main Pärvie fault (reflection R3) and the west dipping reflection R1 in Figs. 5 and 6 have different reflectivity characteristics. The main fault is a weakly reflective structure, while the subsidiary west dipping fault indicates the presence of a strong impedance contrast. Possible explanations for this difference include secondary mineralization, varying fluid content and pressure, anisotropy and thickness of fracture zones. Mineralization along a fault may increase the velocity of the rocks within the fault zone and therefore change the seismic impedance (Jones and Nur, 1982). What type of mineralization that is present depends on the surrounding rocks and the alteration processes which have occurred along the fault. Figure 8 shows the rock type distribution near the Pärvie fault system. Ultramafic intrusive rocks outcrop in different locations. These rocks are mostly exposed near the west dipping fault (reflection R1) at the surface. In the area marked by the rectangle in Fig. 8 these ultramafic bodies are clearly bounded by the fault. This suggests that the west dipping fault cuts these ultramafic intrusions and therefore the fault zone has a potential to be filled by secondary minerals such as silicates, phyllosilicates or calcium that crystallized during or after the post-glacial deformation. The presence of water in the fault can also speed up this process, while the water itself can decrease seismic impedance along the fault (Jones and Nur, 1982).

Jones and Nur (1982) suggest another possibility for strong reflectivity along faults, the existence of high fluid pressure. In order to have a high pore (fluid) pressure along a fault, it is necessary to have a confined structure also along it. This can

SED
7, 537–563, 2015

be accomplished by mylonitic rocks along faults having a tight fabric which eliminate void (pore) spaces and allow the faults to be impermeable structures (Jones and Nur, 1982). In addition, the direction of anisotropy along the faults should be considered to explain their reflectivity. This factor is more important where phyllosilicate minerals such as mica and biotite are present as secondary minerals along the faults. Velocities of seismic waves vary if the waves travel parallel to foliation of the phyllosilicates or perpendicular to them (Jones and Nur, 1982).

The thickness of the west dipping reflection which corresponds to the west dipping fault is in order of 500–800 m while the R3 reflection is much thinner (Figs. 5 and 6). If a fault is still active then this may result in increased fracturing in the subsurface due to displacements along the fault. The thicker the fractured zone, the more seismic reflectivity can be observed. The thickness of the fault R1 appears to decrease with depth (Fig. 6), suggesting that the fracture zone of the fault is larger near to the surface.

The difference between the thicknesses of the fracture zones along the faults is a possible explanation for the difference between the reflectivity of the faults. However, if secondary mineralization has occurred along the faults, then the fault R1 has more capacity to host the secondary minerals than the thinner R3 fault.

6 Discussion

The three steeply dipping faults are imaged down to about 7.5 km in the new dataset while Juhlin et al. (2010) showed four faults in their seismic images down to about 2–3 km. The R2 fault from Juhlin et al. (2010) has not been imaged in our seismic processing. In Fig. 9, the R2 reflection is shown by a dashed line and question marks. The sparsity of the dataset did not allow clear imaging of the R2 fault. If the R1 and R3 faults are extrapolated with their respective dips in Fig. 7, these faults converge at a depth of about 11.5 km (Fig. 9). Figure 9 also shows the location of earthquakes in the area projected onto the migrated and depth converted seismic section. Only well constrained micro-earthquakes within an area of 400 km^2, and with a maximum offset

SED
7, 537–563, 2015

of 10 km perpendicular to the seismic profile, are projected onto the migration plane. A denser cluster of seismic events is located below the imaged faults, suggesting that the intersection at 11.5 km depth of the main Pärvie fault and the west dipping R1 fault is the source of the seismic activity in the area. The geometry of the R1 and R3 faults is uncertain below this depth. It is possible that the main fault (R3) becomes listric at deeper levels, but is currently less seismically active there. The earthquake activities north and south of the study area indicate that this may be the case.

Another scenario is the existence of a flower structure (Juhlin et al., 2010) in which the R1 and R3 faults converge to a master fault at depths of about 11–12 km. We note, however, that the deeper part of such a flower structure would be virtually aseismic, as there are no recorded earthquakes below the cluster in Fig. 9. There are deeper events east of the study area, in better agreement with a listric or generally east dipping fault structure. In addition, the seismicity in the northern and southern sections of the fault does not support a fault wide flower structure but rather an east dipping fault zone (Lindblom et al., 2014).

This paper provides critical site survey information for the DAFNE ICDP drilling proposal. The difference in reflectivity for the reflectors R1 and R3 has strongly influenced the drilling plan. Drilling is now planned to be executed in two phases, with the first phase consisting of drilling two 1 km deep boreholes into the reflectors R1 and R3 and then installing borehole seismometers for monitoring seismicity and other processes. Based on the results from the first two boreholes, a deeper borehole to 2.5 km will be drilled into one of the faults. Combined reprocessing of the two surveys with 3-D swath imaging (e.g. Malehmir et al., 2009) may also help in determining the optimum location for the deep borehole in phase two.

7 Conclusions

The Pärvie fault system was activated during the last glacial retreat in northern Sweden. In order to better understand the geometry of the faults, we carried out

SED
7, 537–563, 2015

a deep seismic survey using dynamite as an explosive source. Although the acquisition parameters resulted in a sparse data set, the quality of the data in terms of signal-to-noise ratio was good. The data were processed following a conventional CDP processing method along a straight line. Three reflections, corresponding to three steeply dipping faults and some sub-horizontal reflections in the subsurface were imaged. The reflections were migrated to their true locations using the Stolt migration method and were traced down to a depth of about 7.5 km. Although weak, the main Pärvie fault is imaged dipping at approximately 65° to the east. A subsidiary, 60° west dipping fault is significantly more reflective. We interpret the subsidiary west dipping fault as consisting of a thicker fracture zone than the main Pärvie fault, explaining the difference in the reflectivity of the faults. Recent earthquakes cluster at a depth of about 11.5 km. The location and depth of the earthquake epicenters are consistent with the intersection of the main fault and the subsidiary fault at depth, assuming the faults are planar. The new seismic survey does not provide any information on the structure of the fault system at greater depth than approximately 8 km. Both a flower structure and the main fault becoming listric in the lower crust are possible crustal structures.

Acknowledgements. The field work has been supported by the Kempefoundations (grant JCK-1202), the Swedish Nuclear Fuel and Waste Management Co. (SKB; Order no. 11149), LKAB (lodging, explosives and blast manager), and Uppsala University. We gratefully acknowledge the support of R. Munier (SKB), C. Dahner, P. Söderman, L. Krekula and L. Kemi (LKAB). O. Ahmadi would like to thank the University of Kurdistan and Ministry of Science, Research and Technology of Iran for their support and funding to study abroad. We also thank the field staff for their devoted work, A. Larsson, E. Nilsson, E. Bjänndal, J. Sandberg, R. Klapp, S. Lindfors, T. Rasmussen from Luleå university of Technology, F. Zhang and I. Lydersen from Uppsala University. Special thanks are given to H. Palm (HasSeis), without whom this study would not have been possible. GLOBE Claritas™ under license from the Institute of Geological and Nuclear Sciences Limited, Lower Hutt, New Zealand was used to process the seismic data. The seismic plots were generated using GMT. Quantum GIS was used to produce the maps.

SED
7, 537–563, 2015

References

Arvidsson, R.: Fennoscandian earthquakes: whole crustal rupturing related to postglacial rebound, Science, 274, 744–746, doi:10.1126/science.274.5288.744, 1996.

Bungum, H. and Lindholm, C.: Seismo- and neotectonics in Finnmark, Kola and the southern Barents Sea, part 2: seismological analysis and seismotectonics, Tectonophysics, 270, 15–28, doi:10.1016/S0040-1951(96)00139-4, 1997.

Bäckstrom, A., Viola, G., Rantakokko, N., Jonsson, E., and Ask, M.: Preliminary results from fault-slip analysis of the Pärvie neotectonic postglacial fault zone, northern Sweden, EGU General Assembly, Vienna, Austria, 7–12 April 2013, EGU2013-1751, 2013.

Edfelt, Å., Sandrin, A., Evins, P., Jeffries, T., Storey, C., Elming, S.-Å., and Martinsson, O.: Stratigraphy and tectonic setting of the host rocks to the Tjårrojåkka Fe-oxide Cu-Au deposits, Kiruna area, northern Sweden, GFF, 128, 221–232, doi:10.1080/11035890601283221, 2006.

Gregersen, S.: Crustal stress regime in Fennoscandia from focal mechanisms, J. Geophys. Res., 97, 11821–11827, doi:10.1029/91JB02011, 1992.

Heidbach, O., Tingay, M., Barth, A., Reinecker, J., Kurfeß, D., and Müller, B.: The World Stress Map database release 2008, doi:10.1594/GFZ.WSM.Rel2008, 2008.

Juhlin, C. and Lund, B.: Reflection seismic studies over the end-glacial Burträsk fault, Skellefteå, Sweden, Solid Earth, 2, 9–16, doi:10.5194/se-2-9-2011, 2011.

Juhlin, C., Elming, S.-Å., Mellqvist, C., Öhlander B., Weihed P, and Wikström A.: 2002, Onshore crustal reflectivity of the Archaean-Proterozoic boundary and comparison with BABEL Lines 2 and 3, northern Sweden, Geophys. J. Int., 150, 180–197, 2002.

Juhlin, C., Dehghannejad, M., Lund, B., Malehmir, A., and Pratt, G.: Reflection seismic imaging of the end-glacial Pärvie Fault system, northern Sweden, J. Appl. Geophys., 70, 307–316, doi:10.1016/j.jappgeo.2009.06.004, 2010.

Juhojuntti, N. and Juhlin, C.: Seismic lower crustal reflectivity and signal penetration in the Siljan Ring area, central Sweden, Tectonophysics, 288, 17–30, 1998.

Juhojuntti, N., Juhlin, C., and Dyrelius, D.: Crustal reflectivity underneath the Central Scandinavian Caledonides, Tectonophysics, 334, 191–210, doi:10.1016/S0040-1951(00)00292-4, 2001.

SED
7, 537–563, 2015

Kuivamäki, A., Vuorela, P., and Paananen, M.: Indications of postglacial and recent bedrock movements in Finland and Russian Karelia (Tech. Rep. No. YST-99). Helsinki, Finland: Geological Survey of Finland, 1998.

Kukkonen, I. T., Olesen, O., Ask, M. V. S., and the PFDP Working Group: Postglacial Faults in Fennoscandia: targets for scientific drilling, GFF, 132, 71–81, doi:10.1080/11035891003692934, 2010.

Kukkonen, I. T., Ask, M. V. S., and Olesen, O.: Postglacial Fault Drilling in Northern Europe: Workshop in Skokloster, Sweden, Scientific Drilling, (11 March 2011), doi:10.2204/iodp.sd.11.08.2011, 2011.

Lagerbäck, R.: Neotectonic structures in northern Sweden, Geol. Foren. Stock. For., 100, 263–269, doi:10.1080/11035897809452533, 1978.

Lagerbäck, R. and Sundh, M.: Early Holocene Faulting and Paleoseismicity in Northern Sweden, Geological Survey of Sweden, 2008.

Lindblom, E. and Lund, B.: Focal mechanisms and the state of stress along the Pärvie end-glacial fault, northern Sweden, in: Lindblom, E., Microearthquake study of end-glacial faults in northern Sweden, Licentiate theses, Uppsala University, Uppsala, Sweden, 2011.

Lindblom, E., Lund, B., Tryggvason, A., Uski, M., Bödvarsson, R., Juhlin, C., and Roberts, R.: Microearthquakes illuminate the deep structure of the endglacial Pärvie fault, northern Sweden, Geophys. J. Int., in review, 2014.

Lund, B. and Zoback, M. D.: Orientation and magnitude of in situ stress to 6.5 km depth in the Baltic Shield, Int. J. Rock Mech. Min., 36, 169–190, doi:10.1016/S0148-9062(98)00183-1, 1999.

Lund, B., Schmidt P., and Hieronymus C.: Stress evolution and fault stability during the Weichselian glacial cycle, TR-09-15, Swedish Nuclear Fuel and Waste Management Co. (SKB), Stockholm, Sweden, 106 pp., 2009.

Malehmir, A., Schmelzbach, C., Bongajum, E., Bellefleur, G., Juhlin, C., and Tryggvason, A.: 3-D constraints on a possible deep > 2.5 km massive sulphide mineralization from 2-D crooked-line seismic reflection data in the Kristineberg mining area, northern Sweden, Tectonophysics, 479, 223–240, 2009.

Mantovani, M. and Scherneck, H.-G.: DInSAR investigation in the Pärvie endglacial fault region, Lapland, Sweden, Int. J. Remote Sens., 34, 8491–8502, 2013.

Mikko, H., Smith, C., Lund, B., Ask, M., Munier, R.: LiDAR-derived inventory of post-glacial fault scarps in Sweden, GFF, in review, 2014.

SED
7, 537–563, 2015

Olesen, O., Blikra, L., Braathen, A., Dehls, J., Olsen, L., Rise, L., Roberts, D., Riis, F., Faleide, J., and Anda, E.: Neotectonic deformation in Norway and its implications: a review, Norwegian J. Geol., 84, 3–34, 2004.

Pascal, C., Stewart, I. S., and Vermeersen, B. L. A.: Neotectonics, seismicity and stress in glaciated regions, J. Geol. Soc. London, 167, 361–362, doi:10.1144/0016-76492009-170, 2010.

Riad, L.: The Pärvie fault, Northern Sweden, Uppsala University. Mineralogy Department of Mineralogy and Petrology, UUDMP Research Report 63, 71 pp., 1990.

Slunga, R. S.: The Baltic Shield earthquakes, Tectonophysics, 189, 323–331, doi:10.1016/0040-1951(91)90505-M, 1991.

Vogel, H., Wagner, B., Rosén, P.: Lake floor morphology and sediment architecture of Lake Torneträsk, Northern Sweden, Geogr. Ann. A, 95, 159–170, doi:10.1111/geoa.12006, 2013.

SED
7, 537–563, 2015

Table 1. Seismic acquisition parameters used during the seismic recording.

Profile length	22 km
Seismic source	Explosive 8.34 kg/shot hole
Geophone	10 Hz
Receiver spacing	25 m
Nominal Shot spacing	400 m
Sampling rate	1 ms
Recording date	Jun 2014

SED
7, 537–563, 2015

Table 2. Seismic data processing steps.

Reading SEGD files and sorting the data	
Geometry setting	
Picking First Arrivals	
Inner trace muting	
Refraction static correction	
Spectral Balancing	SPEQ 10-20-100-150 Hz
Spherical divergence correction	
Band pass filtering	10-20-100-150 Hz
Reflection Residual correction	
FXDECON	7 traces window
Time variant filtering	0–650 ms: high pass 3–70 Hz 655–5000 ms: band pass 15–25-90-120
Velocity analysis	
NMO correction	Constant velocity 13 000 m s^{-1}
Velocity analysis	
First arrival and ground roll muting	
Stacking	
FXDECON	7 traces
Band pass filtering	15-25-90-120 Hz
Migration (Stolt)	

SED
7, 537–563, 2015

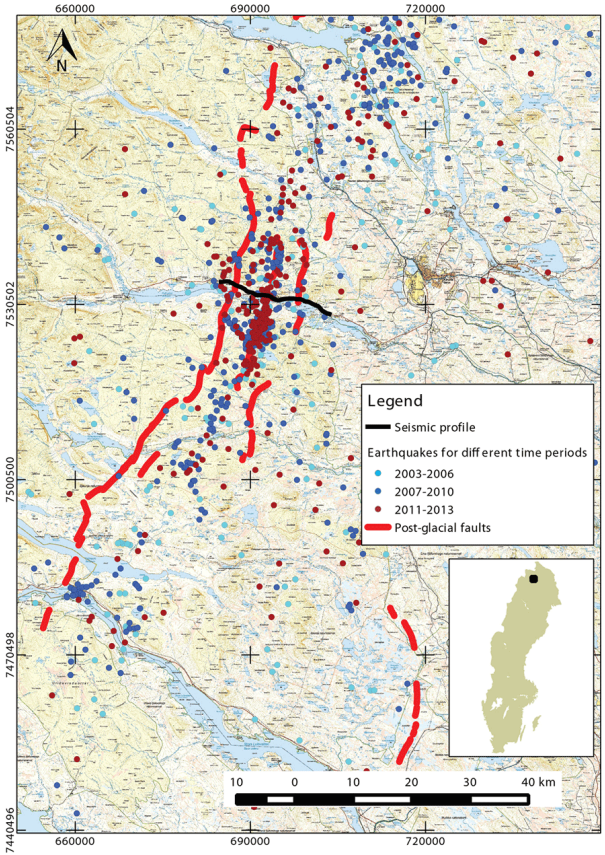

Figure 1. Location of the seismic profile over the Pärvie fault system in northern Sweden. Earthquakes are shown for three different time periods (after Lindblom et al., 2014). Inset shows the location of the Pärvie area in northern Sweden.

SED
7, 537–563, 2015




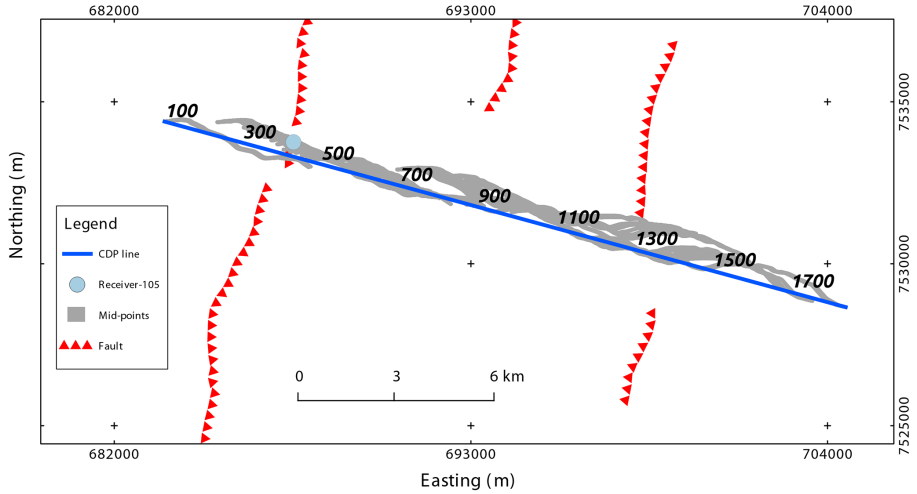

Figure 2. The seismic profile location across the Pärvie fault system. The midpoint distribution shows the sparsity of the data. Location where a weak reflection was recorded in a few shot gathers, corresponding to the main fault, is marked on the map.

SED
7, 537–563, 2015

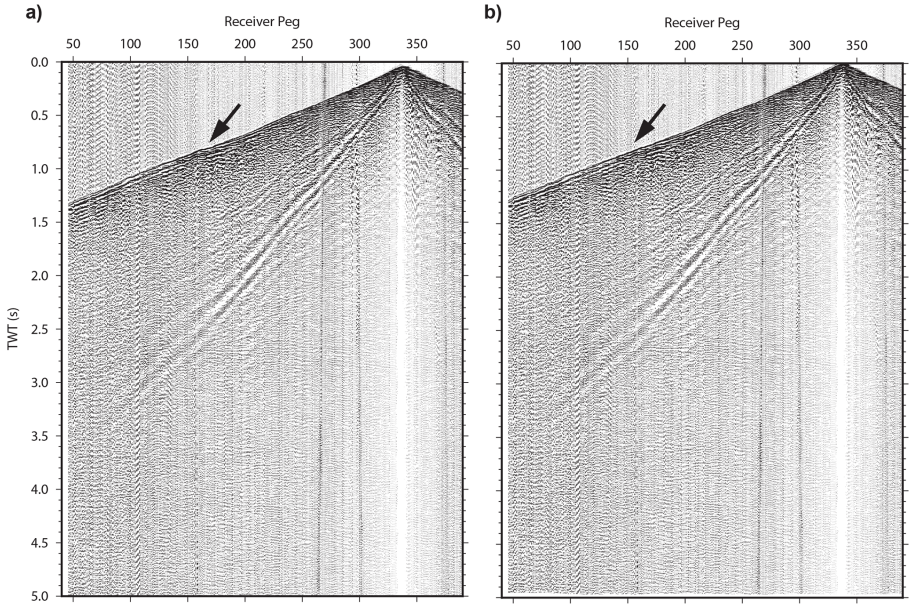

Figure 3. A shot gather **(a)** before refraction static correction **(b)** after the correction. The arrow shows first arrivals which are improved and aligned after static correction.

SED
7, 537–563, 2015

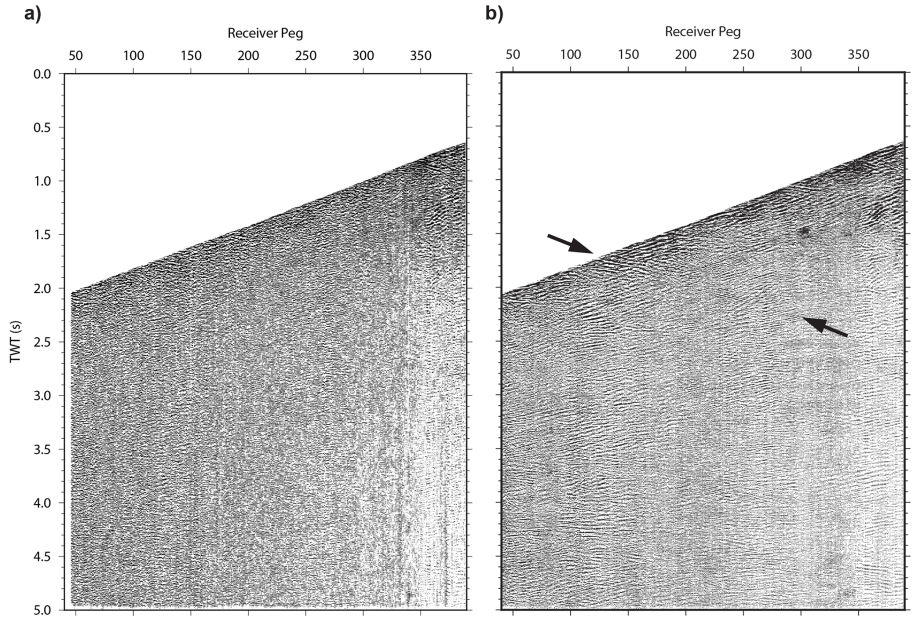

Figure 4. Application of FX-Decon in pre-stack processing **(a)** before **(b)** after FX-Decon. The arrows show an enhanced reflection which is exposed at about receiver peg of 105 at the surface and corresponds to the main east dipping Pärvie fault (see the location of the receiver in Fig. 2).

SED
7, 537–563, 2015

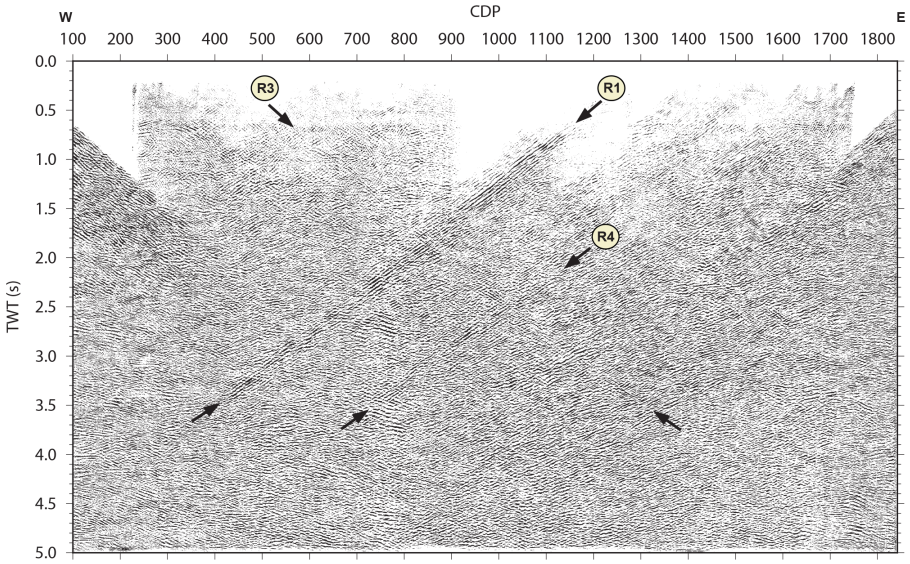

Figure 5. The NMO stacked section. Reflection R1 and R3 correspond to the subsidiary west dipping fault, and the main Pärvie fault respectively. Reflection R4 most likely is another west dipping fault in the subsurface.

SED
7, 537–563, 2015

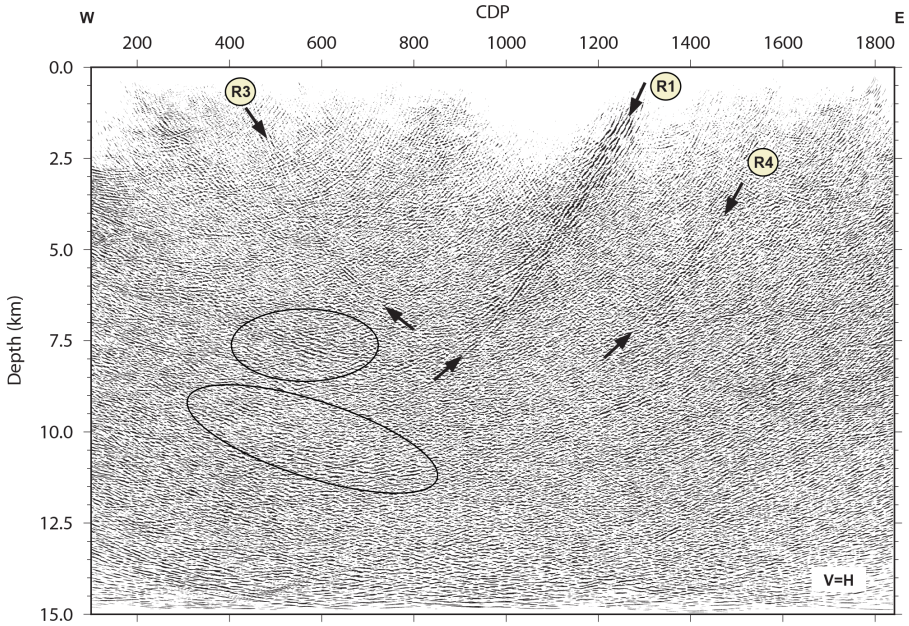

Figure 6. The migrated section. The reflections were migrated to their true locations using a constant velocity of 6000 m s^{-1} approximately.

SED
7, 537–563, 2015

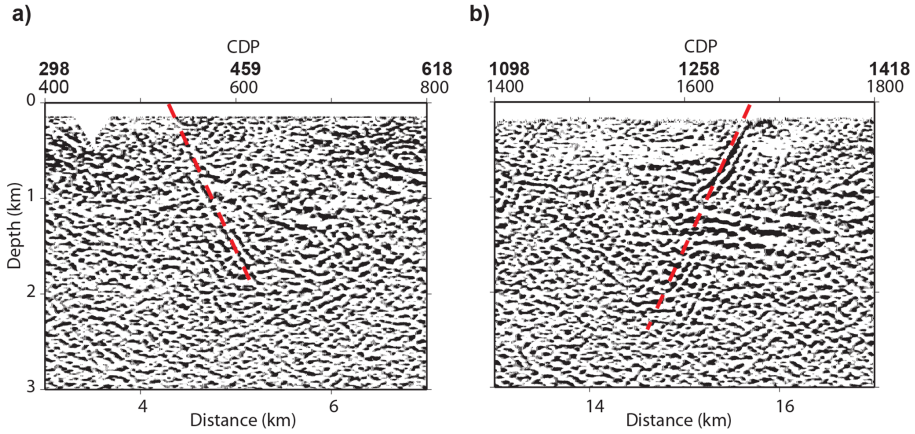

Figure 7. The re-migrated sections of the previous seismic survey (Juhlin et al., 2010) with the velocity model provided by Lindblom et al. (2014). **(a)** The image of the main Pärvie fault (R3) **(b)** the image of the west dipping subsidiary fault (R1). The images show that the R1 and R3 faults dip at about 60 and 65° to the east and the west, respectively. CDP numbers from the new explosive survey are shown in bold. The vertical exaggeration is 1×.

SED
7, 537–563, 2015

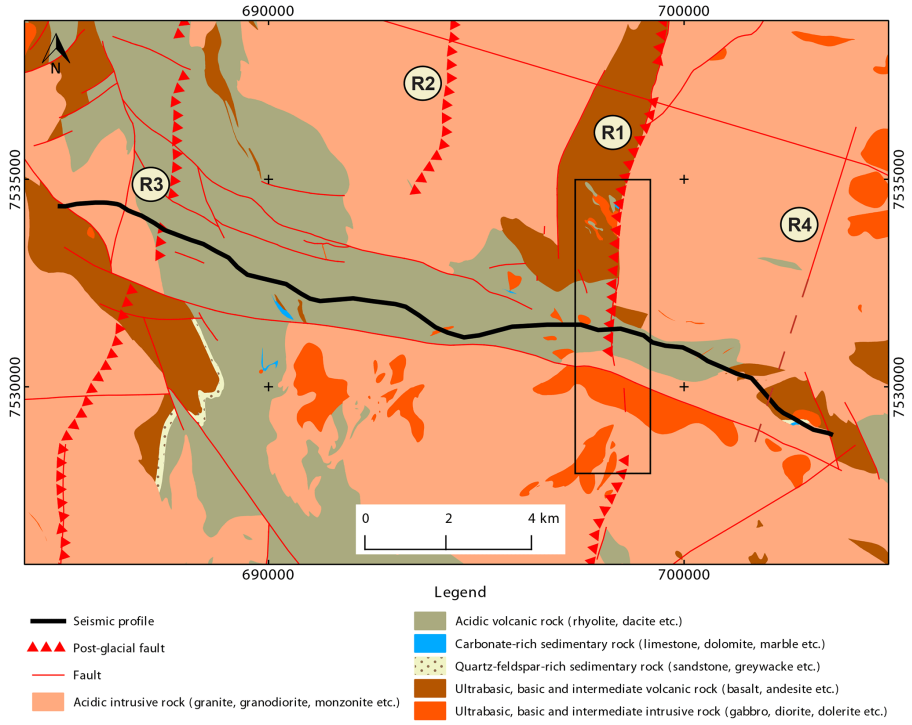

Figure 8. The bedrock geologic map of the area based on Geological survey of Sweden (SGU) database. The rectangle shows where the ultramfic rocks are exposed around the strongly reflective fault R1 (see Fig. 5).

SED
7, 537–563, 2015

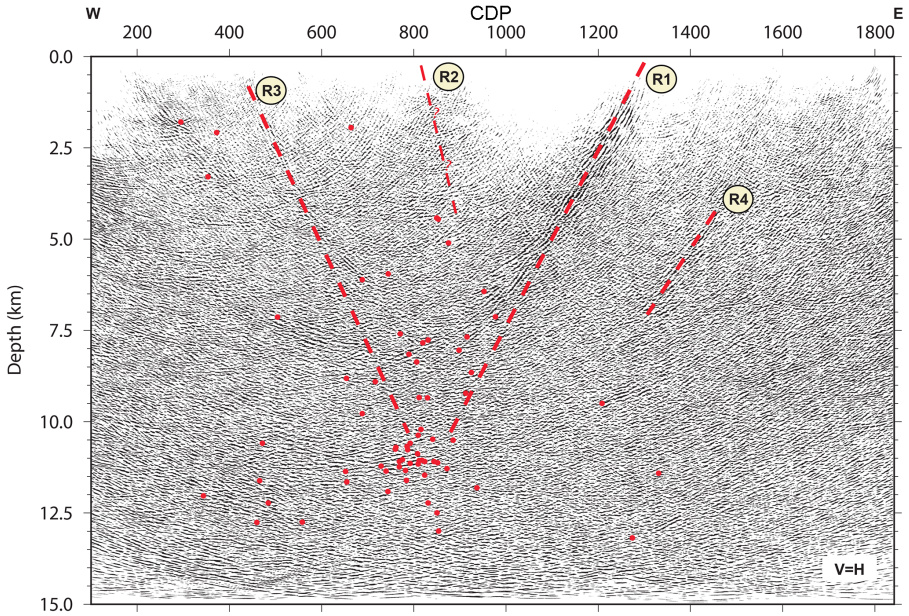

Figure 9. Cross-section of the earthquakes overlaid on the interpreted migrated section. Red dashed lines depict the interpreted faults. Fault R2 was not imaged in the new seismic survey. All events within a maximum offset of 10 km perpendicular to the seismic profile to the north and south are projected onto the CDP plane. A dense cluster of seismic activitiy is located at a depth of about 11.5 km. The listric appearance of the R1 and R3 reflections at depth is most likely due to the migration process and not a feature of the faults. We have interpreted the faults to be planar based on the unmigrated sections.

SED
7, 537–563, 2015